HHS Public Access

Author manuscript

Bone. Author manuscript; available in PMC 2017 August 01.

Published in final edited form as:

Bone. 2016 August ; 89: 7–15. doi:10.1016/j.bone.2016.04.010.

Parallel Mechanisms Suppress Cochlear Bone Remodeling to Protect Hearing

Emmanuel J. Jáuregui, BA[1], **Omar Akil, PhD**[2], **Claire Acevedo, PhD**[1,3], **Faith Hall-Glenn, PhD**[1], **Betty S. Tsai, MD**[4], **Hrishikesh A. Bale, PhD**[3], **Ellen Liebenberg, MS**[1], **Mary Beth Humphrey, MD, PhD**[5], **Robert O. Ritchie, PhD**[3], **Lawrence R. Lustig, MD**[2], and **Tamara Alliston, PhD**[1,2]

[1]Department of Orthopaedic Surgery, University of California, San Francisco

[2]Department of Otolaryngology—Head & Neck Surgery, University of California, San Francisco

[3]Materials Science Division, Lawrence Berkeley National Laboratory, Berkeley, CA

[4]Department of Otorhinolaryngology, University of Oklahoma Health Sciences Center

[5]Department of Medicine, University of Oklahoma Health Sciences Center

Abstract

Bone remodeling, a combination of bone resorption and formation, requires precise regulation of cellular and molecular signaling to maintain proper bone quality. Whereas osteoblasts deposit and osteoclasts resorb bone matrix, osteocytes both dynamically resorb and replace perilacunar bone matrix. Osteocytes secrete proteases like matrix metalloproteinase-13 (MMP13) to maintain the material quality of bone matrix through perilacunar remodeling (PLR). Deregulated bone remodeling impairs bone quality and can compromise hearing since the auditory transduction mechanism is within bone. Understanding the mechanisms regulating cochlear bone provide unique ways to assess bone quality independent of other aspects that contribute to bone mechanical behavior. Cochlear bone is singular in its regulation of remodeling by expressing high levels of osteoprotegerin. Since cochlear bone expresses a key PLR enzyme, MMP13, we examined whether cochlear bone relies on, or is protected from, osteocyte-mediated PLR to maintain hearing and bone quality using a mouse model lacking MMP13 ($MMP13^{-/-}$). We investigated the canalicular network, collagen organization, lacunar volume via micro-computed tomography, and dynamic histomorphometry. Despite finding defects in these hallmarks of PLR in $MMP13^{-/-}$ long bones, cochlear bone revealed no differences in these markers, nor hearing loss as measured by auditory brainstem response (ABR) or distortion product oto-acoustic emissions (DPOAE), between wild type and $MMP13^{-/-}$ mice. Dynamic histomorphometry revealed

Corresponding author: Tamara Alliston, Ph.D., Associate Professor, Department of Orthopaedic Surgery, University of California, San Francisco, 513 Parnassus Avenue, S-1155, San Francisco, CA 94143, tamara.alliston@ucsf.edu, 415-502-6523.

Authors' roles: Study conception: EJ, BST, LRL, TA. Study design: All Authors. Study conduct: EJ, OA, CAS, FHG, BST, HAB. Data analysis and interpretation: All authors. Drafting manuscript: EJ and TA. Revising and approving final version of manuscript: All authors. TA takes responsibility for the integrity of the data analysis.

abundant PLR by tibial osteocytes, but near absence in cochlear bone. Cochlear suppression of PLR corresponds to repression of several key PLR genes in the cochlea relative to long bones. These data suggest cochlear bone uniquely maintains bone quality and hearing independent of MMP13-mediated osteocytic PLR. Furthermore, the cochlea employs parallel mechanisms to inhibit remodeling by osteoclasts and osteoblasts, and by osteocytes, to protect hearing. Understanding the cellular and molecular mechanisms that confer site-specific control of bone remodeling have the potential to elucidate new pathways that are deregulated in skeletal disease.

Keywords

Mouse model; Bone matrix; Collagen; Matrix mineralization; Bone remodeling; Osteocytes; Perilacunar remodeling

1. Introduction

Bone remodeling is a dynamic, continuous process that is vital for skeletal adaptation to the changing mechanical or biological environment, for the repair of bone damage, and for mineral homeostasis. In healthy remodeling, bone resorption is matched by bone deposition to maintain a stable bone mass. Osteoclasts create an acidic microenvironment and secrete proteases to resorb the mineral and organic components of bone matrix. Osteoblasts deposit new organic matrix that undergoes progressive mineralization. Osteocytes coordinate bone remodeling by expressing factors such as RANKL and SOST, potent regulators of osteoclasts and osteoblasts, respectively.

In addition to this regulatory role, osteocytes directly participate in bone remodeling through the process called perilacunar remodeling (PLR)[1–3]. Like osteoclasts, osteocytes create an acidic microenvironment[4,5] and secrete proteases such as matrix metalloproteinase-13 (MMP13) and cathepsin K in the perilacunar space. Like osteoblasts, osteocytes deposit new matrix following this local bone resorption. PLR is essential for the maintenance of bone quality and lacuno-canalicular networks[6]. The extensive, interconnected lacuno-canalicular network provides osteocytes with a significant resorption surface area that is much larger than the periosteal, endosteal, and trabecular surface areas combined[7]. Thus, PLR is a powerful mechanism by which osteocytes can rapidly mobilize calcium to meet demanding metabolic conditions, such as lactation[8]. Although PLR was initially observed over a century ago[9], known then as osteocytic osteolysis, molecular approaches have only recently been applied to understand it[2]. PLR is regulated by parathyroid hormone (PTH) and sclerostin, and likely many other pathways[2,10]. Nonetheless, many questions remain about the physiological role and regulation of PLR, as well as how these processes are disrupted in skeletal disease.

The material quality of bone extracellular matrix (ECM) is biologically regulated and anatomically distinct, such that the elastic modulus of tibia and femur bone ECM is higher than that of calvarial bone. The elastic modulus of cochlear bone ECM is second only to enamel, a unique feature that is essential for hearing[11]. Indeed, a 1.0 GPa decrease in cochlear bone ECM elastic modulus correlates to a 1.84 dB hearing loss[12]. However, the mechanisms that establish such site-specific differences in bone quality are not well defined.

Since we previously implicated MMP13-dependent PLR in the control of bone quality in the appendicular skeleton[6], and in light of cochlear bone's remarkable material properties, we sought to investigate the role of osteocyte-mediated PLR in the cochlea.

The unique form and function of cochlear bone relies, in part, on specialized mechanisms that regulate bone remodeling by osteoclasts and osteoblasts. Cochlear bone remodeling by osteoclasts and osteoblasts occurs at an incredibly low rate, at an overall capsular turnover of 2.1%/year, with nearly full inhibition in the central perilymphatic regions (0.13%/year), compared to 13.9% in the surrounding extracapsular cranial bones[13]. The suppression of osteoclast activity has been convincingly attributed to elevated levels of the osteoclast antagonist osteoprotegerin (OPG). OPG is secreted from the interdental cells of the spiral limbus, with highest concentrations in the perilymph where osteoclast activity is lowest[14]. The suppression of bone remodeling is lost in OPG deficient mice, which have both sensorineural hearing loss due to demyelination of the cochlear nerve[15] and conductive hearing loss due to bony overgrowth of the ear[14]. This phenotype, however, can be ameliorated with bisphosphonate treatment[16].

In spite of the normal suppression of osteoclast function in healthy cochlea, bone quality and hearing are maintained throughout life. Does cochlear bone rely on PLR to maintain bone quality? Or, is turnover of bone by osteocytes also exceptionally low in the cochlea? Answering this question has significant impact for elucidating the mechanisms responsible for hearing loss associated with a number of human skeletal diseases including Paget's disease, fibrous dysplasia (FD), otosclerosis, and osteogenesis imperfecta. Currently, these diseases are largely explained by dysregulation of osteoclasts and osteoblasts. The extent to which osteocytic PLR, mediated by MMP13, is involved in maintaining cochlear bone and ultimately hearing is currently unknown.

We found in mice with a fibrous dysplasia phenotype, that bone overgrowth and hearing loss were most severe in cochlea that exhibit high levels of MMP13 overexpression[17]. Therefore we will test the hypothesis that MMP13-dependent osteocyte-mediated bone remodeling must be carefully regulated in the ear. Therefore, we seek to investigate the cellular and molecular mechanisms that maintain cochlear bone in a mouse model deficient in MMP13, with defective long bone PLR, to evaluate whether the cochlea is uniquely dependent on MMP13-mediated osteocytic PLR to maintain cochlear bone and normal hearing.

2. Materials & Methods

2.1 Mouse Strain

Two-month or five-month-old male mice deficient in the gene for matrix metalloproteinase-13 (MMP13$^{-/-}$) and their wild type (WT) litter mates were used for this study, the generation and phenotype has been previously described[18]. All mice were bred on an FVB/N background. Wild type littermates were used as controls in all experiments. All procedures and animal handling described herein were done according to approved national ethical guidelines and complied with the Institutional Animal Care and Use Committee (IACUC) at the University of California at San Francisco, which approved all protocols.

2.2 Histological Analyses

The histologic analyses employed herein required multiple processing methods. For each assay, at least three non-adjacent sections were examined.

2.2.1 Plastic Sections—For evaluation of sensorineural and bony structures of the cochlea, dissected cochleae were perfused through the round and oval window with 2% paraformaldehyde (PFA) and 2% glutaraldehyde in phosphate buffered saline (PBS) and incubated overnight at 4°C. Cochleae were then rinsed with 0.1M PBS and post fixed in 1% osmium tetroxide for 1 hour prior to immersion in 5% ethylenediaminetetraacetic acid (EDTA) for 2–3 days until sufficiently decalcified. Cochleae were subsequently dehydrated in ethanol and propylene oxide and embedded in Araldite 502 resin (Electron Microscopy Sciences, Fort Washington, PA) for 5 μm sectioning. Sections were stained with Toluidine Blue and mounted in Permount (Fisher Scientific, Houston, TX) on microscope slides. Data from n=3 wild type mice and n=3 $MMP13^{-/-}$ mice were obtained.

2.2.2 Frozen Sections and Immunohistochemistry—Immunohistochemistry was performed on frozen cochlear sections generated as previously described[10]. Briefly, harvested cochleae were perfused through the round and oval windows and fixed in 4% PFA in 0.1M PBS 1–2 hours, rinsed with PBS, decalcified in EDTA, incubated in sucrose overnight, and embedded in Tissue O.C.T. Compound (Sakura Finetek, Torrence, CA). Sections of 12 μm were stored at −20°C until analyzed for immunohistochemistry of MMP13 as described[6]. MMP13 was localized using goat-derived anti-mouse MMP13 primary antibody (AB-8012, Millipore, Billerica, MA) and an HRP-conjugated donkey-anti-goat secondary antibody (SC-1012, Santa Cruz Antibodies, Santa Cruz, CA), followed by signal amplification using the Vectastain Elite kit (Vector Labs, Burlingame, CA) and staining with 3,3'-diaminobenzene. Analysis was performed on cochlea isolated from wild type mice of different ages (E15, E19, P1, P5, P10, P21, and P60) to document the variation of MMP13 expression during development. Data from n=3 wild type mice were obtained.

2.2.3 Histological Analysis of Paraffin Sections—For paraffin sectioning, dissected cochleae, femora, and tibiae were fixed in 4% PFA in PBS pH 7.4 and then incubated in 10% di- and trisodium EDTA for 7–10 days until fully decalcified, followed by serial ethanol dehydration and paraffin embedding. Paraffin sections (7 μm thick) were generated using a microtome (Leica Microsystems, Buffalo Grove, IL) for polarized light microscopy and Ploton silver stain.

2.2.4 Polarized Light Microscopy—Polarized light microscopy was performed on paraffin embedded sections stained in a saturated aqueous solution of picric acid (Cat# P6744, Sigma-Aldrich, St. Louis, MO) and 0.1% sirius red (Cat# 365548, Sigma-Aldrich, St. Louis, MO) as previously described[19], then dehydrated, cleared, and mounted. On microscopy, polarized filters were rotated to achieve the maximum birefringence before capturing an image. Birefringence was quantified from collected images using OrientationJ, an ImageJ plug-in, as previously described[20]. Data were collected from n=4 cochleae for each group, and from n=3 femora for each group.

2.2.5 Ploton Silver Stain—To visualize the lacuno-canalicular network on cochleae and femora, paraffin embedded sections were deparaffinized and rehydrated, then incubated in two-parts 50% silver nitrate and one-part 1% formic acid (Cat# A119^{p}-4, Fisher Scientific, Fairlawn, NJ) with 2% gelatin (Cat# G8-500, Fisher Scientific, Fairlawn, NJ) solution for 55 minutes. Stained slides were then washed in 5% sodium thiosulfate (Cat# 5-3946, Baker Chemicals, Philipsburg, NJ) for 10 minutes and subsequently dehydrated, cleared, and mounted. Analysis and quantification of the lacuno-canalicular area was performed on images acquired at 100× magnification with ImageJ by thresholding gray-scale images for darker, silver stained lacunae and canaliculi. The resulting area was normalized to total bone area analyzed for each image captured. Data was collected from n=4 cochleae from each group. For femora, in which we had previously characterized the MMP13-dependent defects in the lacuno-canalicular network[6], analyses were performed on bones from n=3 MMP13$^{-/-}$ and n=2 wild type mice.

2.2.6 Dynamic Histomorphometry of Mineralized Bone Sections—MMP13$^{-/-}$ mice and their wild-type littermates were given two intra-peritoneal injections of calcein (0.01 mg/g; Sigma-Aldrich, St. Louis, MO) in a 2% sodium bicarbonate and PBS solution, 5 days apart and two days prior to euthanasia as described[6]. Dissected cochleae and tibiae were fixed overnight in 10% buffered formalin, rinsed, serially dehydrated in ethanol, and embedded in methyl methacrylate[21]. Sections were obtained with a sectioning saw (Buehler Isomet: Low-speed Saw, Lake Bluff, IL) and then sanded down with increasing grades of sandpaper until the desired thickness of roughly 100 μm to 200 μm was achieved; images were then taken using confocal microscopy (Nikon Eclipe E800, Tokyo, Japan). The number of calcein-labeled lacunae was assessed with a 40× optical objective. The number of calcein-labeled lacunae was divided by total number of lacunae in the section to provide a percentage. Data was collected from sections of tibia and cochlea from n=3 mice.

2.3 Computed Tomography

2.3.1 Micro-Computed Tomography—Sagittal sections of mice heads were scanned by micro-CT (VivaCT-40, Scanco Medical, Bassersdorf, Switzerland). After identification of the cochlea on a scout view, image acquisition consisted of 418 slices encompassing the cochlea at 10.5mm voxel size in all three axes. For each 180degrees, 10000 projections were taken. Settings included: Voxel size Integration time 346, with E(KVp) of 55 and I(uA) of 145, uScaling 4096. Evaluation of 220 slices that included the ossicular chain was performed and 2D and 3D reconstructions of these slices were generated Scanco software. Cochlear bone was excluded from the analysis to allow visualization of the internal bone structures including the ossicular chain. The images were segmented using a low pass filter to remove noise, and a threshold was generated to edit regions of the cochlea. The same threshold was used for all samples (Sigma 0.70, support 1, threshold 280). Data from n=3 wild type mice and n=3 MMP13$^{-/-}$ mice were obtained.

2.3.2 Synchrotron x-Ray Micro-Computed Tomography—Cochleae from MMP13$^{-/-}$ and wild type mice were scanned to visualize osteocyte lacunar volume and quantify mineralization with synchrotron x-ray microtomography (SμCT). SμCT was performed at beamline 8.3.2 of the Advanced Light Source (ALS) at the Lawrence Berkeley

National Laboratory. Scanning experiments were conducted with an incident x-ray energy at 19–20 keV in monochromatic mode and an exposure time of 800–1100 ms, with a 5× lens resulted in a subsequent spatial resolution of 1.3 μm per voxel (camera PCO Edge). Slices taken over 180° sample rotation were reconstructed with Octopus (Octopus v8; IIC UGent, Zwijnaarde) before being analyzed with ImageJ (Rasband, W.S., ImageJ, US National Institutes of Health, Bethesda) and AVIZO software (FEI, Hillsboro, OR). Bone mineral density was calculated from the mass attenuation coefficients (grayscale values) of voxels present in the studied volume.

Segmentation of lacunar volume in the bone samples was performed with ImageJ. Quantitative analyses of lacunar volume were computed with AVIZO. After converting image datasets to 8-bit format and smoothing with a median3D filter, images were segmented[22] into osteocyte lacunae by using a masking procedure (thresholding). From the binary lacunar mask, individual lacunae were labeled and quantified in term of 3D volume in AVIZO. The volume of interest of osteocyte lacunae is within the range of 50 to 500 μm^3. Porosities with a volume smaller than 50 μm^3 were considered as noise and not taken into account in the quantification. Data from n=3 wild type mice and n=3 $MMP13^{-/-}$ mice were obtained.

2.4 Auditory Evaluations

Auditory brainstem response (ABR) threshold testing and distortion product oto-acoustic emissions (DPOAE) testing were performed in a sound proof chamber as previously described[17] on mice >5 months of age, but <7 months of age to avoid possibility of acquired age-related hearing loss[23]. Briefly, on anesthetized mice electrodes were placed for ABR testing on the left (test) and right (ground) ears. Four different stimuli were presented using the TDT BioSig III system (Tucker-Davis Technologies, Alachua, FL): click stimulus for 5 ms duration, tone pips of 8, 16, and 32 kHz for 10ms duration. Twenty millisecond EEG segments were recorded. The lowest level at which distinct waveforms could be visualized above noise floor was determined to be the threshold level. This was then confirmed with data analysis performed via MATLAB (MathWorks, Torrence, CA). Data from n=5 wild type mice and n=10 $MMP13^{-/-}$ mice were obtained.

DPOAEs, briefly, were obtained via a probe placed in the external auditory canal. Two-toned stimuli with a standard frequency ratio (f_2/f_1=1.25) synthesized using SigGen software were presented at equal levels via two separate speakers (EC1; Tucker Davis Technologies, Alachua, FL). A microphone (ER10B+, Etymotics Research, Elk Grove Village, IL) within the probe recorded the DPOAE response. For each stimulus set, DPOAE amplitude level at $2f_1-f_2$ was extracted and sound pressure levels for data points 100 Hz above and below the DPOAE frequency were averaged for noise floor measurements. Data from n=5 wild type and n=10 $MMP13^{-/-}$ mice were obtained.

2.5 RNA Isolation and Reverse Transcription Quantitative PCR (RT-qPCR) Analyses

Bones (femora, tibiae, and cochleae) were dissected from wild type mice at postnatal day 60, cleaned of soft tissue, and flushed with PBS by syringe or centrifuged to remove bone marrow. Bones were immediately frozen in liquid nitrogen and pulverized using a liquid

nitrogen-cooled mortar and pestle. Tissue was subsequently transferred into 650 mL of Trizol solution (Life Technologies, Grand Island, NY). Following the Trizol and chloroform extractions, further RNA purification was achieved with Qiagen RNeasy and on-column DNase-1 digestion (Qiagen, Valencia, CA), as per manufactures instructions. Isolated RNA was reverse transcribed into cDNA with iScript random hexamer primers (Bio-Rad, Hercules, CA) as instructed by the manufacturer with review of melt curves to ensure quality. Quantitative PCR was done with iQ SYBR Green Supermix (Bio-Rad 170-8882), via the iQ5 Real Time PCR (Bio-Rad) (Supplemental Figure 2 for primer sequences). The relative expression of each gene was calculated using the Delta-Delta-CT method as previously detailed[24], with mouse GAPDH used as the internal control gene. Data from n=6 wild type FVB/N mice were obtained.

2.6 Replicates and Statistical Analyses

All statistical differences were computed using the student's t-test for data that was normally distributed. For data that were not normally distributed, such as DPOAE and ABR data, non-parametric Wilcoxon sum-rank tests were performed. Statistical significance is defined as $p<0.05$. As indicated above and in the Figure Legends, at least 3 biological replicates (individual mice) were used, except in the case of the previously characterized lacuno-canalicular network analysis of WT vs. MMP13$^{-/-}$ tibia, where one group had an n=2 but still showed statistically significant differences that were consistent with our prior observations[6]. In all cases, more than 3 technical replicates were used for analyses. For example, for histological analyses, data were gathered from at least 3 non-consecutive sections per bone.

3. Results

3.1 Analysis of the developmental regulation of MMP13 expression in cochlear bone

Immunohistochemistry (IHC) was performed to examine the spatiotemporal localization of MMP13 protein in the cochlea throughout development. Embryonically and immediately after birth, cochleae express negligible amounts of MMP13 protein (Figure1A and 1B, E15, E19, P1). During endochondral ossification of cochlear bone, MMP13 is expressed at postnatal day 5 (Figure 1A and B, P5), coincident with chondrocyte hypertrophy. MMP13 expression declines throughout P10 and P21, as the cartilage template is replaced by bone. MMP13 expression increases again in the mature cochlea, with maximal levels observed at P60 in the perilacunar regions surrounding osteocytes in the mid-cortical layer of the cochlear bone. The specificity of MMP13 localization is confirmed by the absence of cochlear bone staining in MMP13 IHC of MMP13$^{-/-}$ cochleae (Supplemental Figure 3) or in control IgG IHC of wild type cochleae (Figure 1A, P60 IgG Control), despite some background staining of cochlear sensorineural tissues in all conditions. Thus, MMP13 expression is developmentally and spatially regulated in the cochlea, with perilacunar localization in mature mid-cortical cochlear bone. This expression pattern resembles that observed in mid-cortical bone of the femur, where MMP13 is critical for osteocyte-mediated perilacunar remodeling and the proper maintenance of bone quality[6]. The lack of mRNA level differences at different stages of development suggests post-translational regulation of mRNA to subsequent protein expression (Supplemental Figure 1).

3.2 Hearing and structural anatomy of the MMP13-deficient cochlea

Given the importance of bone quality in hearing, we sought to determine the effect of MMP13 deficiency on the ear and hearing. Cochleae of MMP13$^{-/-}$ mice show no signs of aberrant bony development. Reconstructed micro-computed tomography (micro-CT) images of MMP13$^{-/-}$ cochleae and ossicular bones (Figure 2A) reveal normal bony anatomy without gross deformities. Vital cochlear structures, such as the organ of Corti and the spiral ganglion, are also unaffected by MMP13 deficiency by histologic observation (Figure 2B).

In spite of apparently normal bony structures of the ear, defects in cochlear bone quality cause hearing loss[12]. Because MMP13 maintains bone quality in the appendicular skeleton and is expressed in cochlear bone, we hypothesized that MMP13 deficiency would impair cochlear bone quality and hearing. To functionally evaluate hearing in MMP13$^{-/-}$ mice we measured the auditory brainstem response (ABR). The ABR thresholds for MMP13$^{-/-}$ mice did not differ significantly from wild type mice in response to multi-frequency click- or frequency-specific stimuli at 8, 16, or 32 kHz (Figure 3A). Distortion product oto-acoustic emission (DPOAE) testing assesses outer hair cell and efferent auditory function. MMP13$^{-/-}$ mice showed no significant differences in DPOAEs relative to their wild type littermates (Figure 3B), indicating that outer hair cell function of MMP13$^{-/-}$ mice is also normal. To test for the possibility that MMP13 deficient mice may be more susceptible to age-related hearing loss, the same tests were performed on mice ≥5-months old. Though ABR thresholds and DPOAE values were more variable in older MMP13$^{-/-}$ mice than in wild-types, no significant differences in hearing were detected at either time point, demonstrating that MMP13 is not required for hearing (data shown is for mice ≥5-months old).

3.3 The hallmarks of perilacunar remodeling are disrupted in femora without MMP13; cochleae, however, maintain normal phenotype

The normal hearing of MMP13 deficient mice raised several questions about the role of osteocyte-mediated perilacunar remodeling in the cochlea. We, therefore, compared the effect of MMP13 deficiency on perilacunar remodeling between the cochlea and the femur, where MMP13 is essential for PLR.[6].

In wild type femora, polarized light microscopy reveals aligned collagen fibers at sites of MMP13 expression in cortical bone (Figure 4F). In the same area of MMP13$^{-/-}$ femora, collagen fibers are disorganized with a more heterogeneous alignment (Figure 4G). However, in cochleae from the same mice, collagen fibrils are aligned in both wild type and MMP13$^{-/-}$ cochlear bone matrix, such that the two groups are qualitatively and quantitatively indistinguishable (Figure 4B–D). Therefore, unlike bones of the appendicular skeleton, cochlear bone matrix organization is maintained independently of MMP13.

Perilacunar remodeling maintains the lacunar-canalicular network. Deficiency in MMP13 or other proteases required for perilacunar remodeling causes a reduction in the lacunar size and lacunar canalicular area. Histological analysis of the canalicular network revealed that MMP13$^{-/-}$ femora have shorter, blunted canalicular projections radiating from osteocyte lacunae relative to wild type femora (Figure 5D–E). Quantification of the lacuno-canalicular area of MMP13$^{-/-}$ femora, normalized to bone area, show a 44% reduction in total lacuno-

canalicular area when compared to wild type littermates, (Figure 5F, p=0.0007). The canalicular network in cochlear bone is qualitatively distinct from that in femora (Figure 5A–B). However, MMP13-dependent differences in lacuno-canalicular area in cochlear bone were not apparent in 2D histologic analyses (Figure 5C, p >0.05).

3.4 Genes associated with perilacunar remodeling have reduced expression in the cochlea

The MMP13-independence of cochlear bone canalicular and collagen organization raises the question of whether the cochlea possesses specialized mechanisms to suppress bone remodeling—either by osteocytes or osteoclasts—to protect hearing. The suppression of osteoclast-mediated remodeling results from high levels of OPG expressed by multiple cochlear structures and dispersed in the perilymph[25]. Loss of OPG causes catastrophic remodeling of the cochlear bone and obliterates hearing[14]. Therefore, we sought to determine if the cochlear expression of MMP13 or other PLR enzymes differed relative to other sites where PLR is active. As expected, cochleae express elevated levels of OPG relative to other bones (Figure 6A). The expression of ATP6V1G1 and MMP14 did not differ among tibia, femur, or cochlea. However, the remaining enzymes implicated in PLR, including the expression of the MMP13, ATP6V0D2, and Cathepsin K, is significantly reduced relative to bones of the appendicular skeleton. Therefore, the cochlea possesses a distinct mechanism for the coordinated suppression of several key PLR enzymes to protect hearing from bone remodeling.

3.5 Osteocyte-mediated perilacunar remodeling is suppressed in cochlear bone

The integrity of cochlear bone in MMP13 deficient mice may reflect the reliance of cochlear perilacunar remodeling on other enzymes, such as MMP14 or MMP2. Alternatively, cochlear bone may be protected from perilacunar remodeling by osteocytes, just as it is protected from osteoclast-mediated remodeling. Cochlear bone has a paucity of osteoclasts. Sorenson used dynamic histomorphometry, with fluorochrome labels to describe the low bone formation rate of evolving secondary osteons in cochlear bone, relative to long bones and surrounding cranial bones[26]. Not only is fluorochrome incorporated into newly formed bone matrix deposited by osteoblasts, but also in the bone matrix deposited by osteocytes that are actively undergoing perilacunar remodeling[21]. Relative to tibia, where 31% of osteocyte lacunae in the cortical bone are calcein positive, only 9.1% of cochlear bone lacunae are calcein positive (Figure 6D). These data suggest that the maintenance of cochlear bone is independent of MMP13, at least in part due to the unique down-regulation of osteocyte-mediated perilacunar remodeling in cochlear bone.

In order to more rigorously evaluate the effect of MMP13 deficiency on lacunar size, we employed x-ray tomographic microscopy (XTM), which visualizes and quantifies lacunar distribution and size in three-dimensional space. We examined the lacunar volume in the cochlea of postnatal day 60. The average lacunar volume of $MMP13^{-/-}$ mice (Figure 7C) did not differ compared to wild type (Figure 7B) cochlear bone when plotted and analyzed (Figure 7D, p>0.05).

4. Discussion

Our data suggest cochlear bone uniquely maintains bone matrix quality and hearing independent of MMP13-mediated osteocytic PLR. We show that, although MMP13 is expressed from embryonic to adult cochlea, MMP13$^{-/-}$ cochleae show neither defects in structural formation, collagen organization, size of cochlear osteocyte lacunae, nor changes in the canalicular network organization, despite seeing defects in these PLR hallmarks in the long bones of the same animals. These data suggest the cochlea, in addition to suppressing the activity of osteoclast- and osteoblast-mediated remodeling, also has diminished osteocyte-mediated PLR, possibly to preserve hearing. Additionally, these findings highlight the importance of site-specific cellular and molecular mechanisms involved in the regulation of bone remodeling tailored to site-specific functions.

Under normal circumstances, bone mass and quality adapt to the changing mechanical and physiological demands placed on the organism. PLR, or osteocytic osteolysis, was formally described in hibernating and lactating animals[10,27,28], whereby the osteocyte locally resorbs the perilacunar mineral matrix in order to maintain homeostatic ion concentrations. Later, osteocytes deposit new bone matrix when the physiologic demand has subsided[29]. Loss of MMP13 diminishes the structural characteristics of bone by disrupting PLR, resulting in heterogeneous mineralization, abnormalities of cortical bone collagen organization, and canalicular network disorganization, together reducing the fracture toughness of bone[6]. However, as the data here suggest, the regulatory mechanisms that control PLR, and thus bone quality, are not uniform across the entire skeleton. Cochlear bone, as part of the specialized sensory organ for hearing, is capable of maintaining bone mass and quality independent of MMP13. Our results suggest that the cellular mechanisms necessary for PLR are down-regulated in the cochlea, in addition to those of osteoclast-mediated bone remodeling.

Therefore, rather than supporting a single mechanism for bone remodeling across the entire skeleton, this study suggests the presence of unique bone-specific mechanisms that control ECM quality; in particular for the cochlea, when considering the importance of cochlear bone quality for hearing. Diseases that dysregulate bone remodeling in the ear can result in hearing loss. For example, fibrous dysplasia (FD), which leads to cochlear bone overgrowth and increased MMP13 expression in the cochlea, can severely impact hearing[12,17]. The extremely high levels of MMP13 in the cochleae of FD[17] mice highlights the important need to control MMP13 expression in order to conserve cochlear bone quality and ultimately hearing. Previous work has demonstrated the tight relationship between ECM quality and hearing; namely, every 1GPa increase in the elastic modulus of cochlear bone results in a 1.84 dB decrease in the ABR threshold[12]. Additionally, the unique material properties of the cochlea are preserved throughout a variety of species and taxa, therefore the presence of redundant, evolutionarily conserved mechanisms, as we have seen to protect hearing, is not entirely surprising[30].

As for the mechanisms responsible for the unique regulation and material properties of cochlear bone ECM, the spiral ligament, the perilymphatic soft tissues and other structures within the cochlea have been shown to secrete high levels of OPG, which inhibit RANKL-

induced osteoclast activity to preserve cochlear bone[25]. Dysregulation of this system leads to bony overgrowth and can result in both conductive and sensorineural hearing loss[15]. This soft-tissue-to-bone crosstalk also offers site-specific regulation in the appendicular skeleton, where muscle derived factors regulate bone and vice versa[31–33]. In the case of the cochlea, loss of the paracrine signals from soft tissue within the cochlea leads to ossicular bone thinning and progressive hearing loss[34].

In considering additional potential mechanisms, it is important to note the anatomical location of the cochlea. The cochlea, along with some of the other craniofacial bones, experiences lower amplitude mechanical loading[35], leading to potentially less microdamage. These low levels of mechanical stimulation or microdamage accumulation may also contribute to the reduced levels of PLR in cochlear bone[36,37]. Additionally, although we assessed several key enzymes implicated in PLR, others may also participate, particularly if they compensate for the lower levels of MMP13.

Cochlear bone matrix material properties are distinct and evolutionarily conserved across taxa, demonstrating their importance. Surgical experience and experimental analysis has revealed that the cochlea is one of the hardest bones in the body[12]. Uniquely, for the function of the cochlea to be maintained, the anatomical relationships between the ossicular chain and the cochlea need to be preserved for proper sound conduction from the outside world to the central nervous system. The revelation that the cochlea does not distinctly rely on PLR for bone maintenance is surprising, especially when considering the cochlea also suppresses osteoclast-mediated remodeling. We add to the current understanding of the unique regulatory mechanisms in the cochlea new evidence to suggest that suppression of bone remodeling in the cochlear bone includes not only osteoclasts and osteoblasts, but also osteocytes. By expanding our understanding of site-specific bone regulation, it may be possible to use targeted therapies to treat bone-remodeling diseases that affect hearing or systemic diseases such as osteoporosis with precision therapies such as cathepsin-K inhibitors and anti-sclerostin antibodies—without potentially compromising cochlear bone quality, and ultimately, hearing.

Supplementary Material

Refer to Web version on PubMed Central for supplementary material.

Acknowledgments

The authors gratefully acknowledge the help from summer students and undergraduates. This research was supported by Hearing Research Inc. (TA, LRL), NIH-NIDCR R01 DE019284 (TA), NIH-NIAMS P30 AR066262-01 (TA), UNCF – Merck Postdoctoral Scholar Fellowship (FHG), AAO-HNS CORE Resident Research Award (BST), NIH R03 DE016868 (TA) and the Deafness Research Foundation (TA).

REFERENCES

1. Qing H, Bonewald LF. Osteocyte remodeling of the perilacunar and pericanalicular matrix. Int J Oral Sci. 2009; 1(2):59–65. [PubMed: 20687297]
2. Teti A, Zallone A. Do osteocytes contribute to bone mineral homeostasis? Osteocytic osteolysis revisited. Bone. 2009; 44(1):11–16. [PubMed: 18977320]

3. Bellido T. Osteocyte-driven bone remodeling. Calcif Tissue Int. 2014; 94(1):25–34. [PubMed: 24002178]
4. Kogawa M, Wijenayaka AR, Ormsby RT, et al. Sclerostin Regulates Release of Bone Mineral by Osteocytes by Induction of Carbonic Anhydrase 2. J Bone Miner Res. 2013; 28(12):2433–2435. [PubMed: 24166807]
5. Wysolmerski JJ. Osteocytes remove and replace perilacunar mineral during reproductive cycles. Bone. 2013; 54(2):230–236. [PubMed: 23352996]
6. Tang SY, Herber R-P, Ho S, Alliston T. Matrix Metalloproteinase-13 is Required for Osteocytic Perilacunar Remodeling and Maintains Bone Fracture Resistance. J Bone Miner Res. 2012; 27(9): 1936–1950. [PubMed: 22549931]
7. Bonewald LF. The Amazing Osteocyte. J Bone Miner Res. 2011; 26(2):229–238. [PubMed: 21254230]
8. Wysolmerski JJ. Osteocytic osteolysis: time for a second look? Bonekey Rep. 2012 Oct.1:229. [PubMed: 24363929]
9. Recklinghausen F. Untersurchungen uber Rachitis and Osteomalacia. Jena: Gustav Fischer. 1910
10. Wysolmerski JJ. Osteocytes Remove and Replace Perilacunar Mineral during Reproductive Cycles. Bone. 2014; 54(2):230–236. [PubMed: 23352996]
11. Currey JD. The design of mineralised hard tissues for their mechanical functions. J Exp Biol. 1999; 202(Pt 23):3285–3294. [PubMed: 10562511]
12. Chang JL, Brauer DS, Johnson J, et al. Tissue-specific calibration of extracellular matrix material properties by transforming growth factor-b and Runx2 in bone is required for hearing. EMBO Rep. 2010 May.:1–7. [PubMed: 20033081]
13. Frisch T, Overgaard S, Sørensen MS, Bretlau P. Estimation of volume referent bone turnover in the otic capsule after sequential point labeling. Ann Otol Rhinol Laryngol. 2000; 109(1):33–39. [PubMed: 10651409]
14. Zehnder AF, Kristiansen AG, Adams JC, Kujawa SG, Merchant SN, Mckenna MJ. Osteoprotegrin Knockout Mice Demonstrate Abnormal Remodeling of the Otic Capsule and Progressive Hearing Loss. Laryngoscope. 2008; 116(2):201–206. [PubMed: 16467704]
15. Kao SY, Kempfle JS, Jensen JB, et al. Loss of osteoprotegerin expression in the inner ear causes degeneration of the cochlear nerve and sensorineural hearing loss. Neurobiol Dis. 2013; 56:25–33. [PubMed: 23607938]
16. Kanzaki S, Takada Y, Ogawa K, Matsuo K. Bisphosphonate therapy ameliorates hearing loss in mice lacking osteoprotegerin. J Bone Miner Res. 2009; 24(1):43–49. [PubMed: 18715136]
17. Akil O, Hall-Glenn F, Chang J, et al. Disrupted bone remodeling leads to cochlear overgrowth and hearing loss in a mouse model of fibrous dysplasia. PLoS One. 2014; 9(5):e94989. [PubMed: 24788917]
18. Stickens D, Behonick DJ, Ortega N, et al. Altered endochondral bone development in matrix metalloproteinase 13-deficient mice. Development. 2004; 131(23):5883–5895. [PubMed: 15539485]
19. Montes GS, Junqueira LC. The use of the Picrosirius-polarization method for the study of the biopathology of collagen. Mem Inst Oswaldo Cruz. 1991; 86(Suppl 3):1–11. [PubMed: 1726969]
20. Rezakhaniha R, Agianniotis a, Schrauwen JTC, et al. Experimental investigation of collagen waviness and orientation in the arterial adventitia using confocal laser scanning microscopy. Biomech Model Mechanobiol. 2012; 11(3–4):461–473. [PubMed: 21744269]
21. Qing H, Ardeshirpour L, Divieti Pajevic P, et al. Demonstration of osteocytic perilacunar/ canalicular remodeling in mice during lactation. J Bone Miner Res. 2012; 27(5):1018–1029. [PubMed: 22308018]
22. Dong P, Haupert S, Hesse B, et al. 3D osteocyte lacunar morphometric properties and distributions in human femoral cortical bone using synchrotron radiation micro-CT images. Bone. 2014; 60:172–185. [PubMed: 24334189]
23. Zheng QY, Johnson KR, Erway LC. Assessment of hearing in 80 inbred strains of mice by ABR threshold analyses. Hear Res. 1999; 130(1–2):94–107. [PubMed: 10320101]
24. Schmittgen TD, Livak KJ. Analyzing real-time PCR data by the comparative C T method. Nat Protoc. 2008; 3(6):1101–1108. [PubMed: 18546601]

25. Zehnder AF, Kristiansen AG, Adams JC, Merchant SN, McKenna MJ. Osteoprotegerin in the inner ear may inhibit bone remodeling in the otic capsule. Laryngoscope. 2005 Jan.115:172–177. [PubMed: 15630389]
26. Sorensen MS, Jorgensen MB, Bretlau P. Remodeling patterns in the bony otic capsule of the dog. Ann Otol Rhinol Laryngol. 1991; 100(9 I):751–758. [PubMed: 1952670]
27. Haller AC, Zimny ML. Effects of hibernation on interradicular alveolar bone. J Dent Res. 1977; 56(12):1552–1557. [PubMed: 277478]
28. Steinberg B, Singh IJ, Mitchell OG. The effects of cold-stress. Hibernation, and prolonged inactivity on bone dynamics in the golden hamster, Mesocricetus auratus. J Morphol. 1981; 167:43–51. [PubMed: 7241597]
29. Cullinane DM. The role of osteocytes in bone regulation: Mineral homeostasis versus mechanoreception. J Musculoskelet Neuronal Interact. 2002; 2(3):242–244. [PubMed: 15758444]
30. Currey JD. Mechanical properties of bone tissues with greatly differing functions. J Biomech. 1979; 12(4):313–319. [PubMed: 468855]
31. Yakar S, Rosen CJ, Beamer WG, et al. Circulating levels of IGF-1 directly regulate bone growth and density. J Clin Invest. 2002; 110(6):771–781. [PubMed: 12235108]
32. DiGirolamo DJ, Kiel DP, Esser KA. Bone and Skeletal Muscle: Neighbors With Close Ties. J Bone Miner Res. 2013; 28(7):1509–1518. [PubMed: 23630111]
33. Waning DL, Guise TA. Cancer-associated muscle weakness: What's bone got to do with it? Bonekey Rep. 2015 May.4:691. [PubMed: 25992285]
34. Kanzaki S, Ito M, Takada Y, Ogawa K, Matsuo K. Resorption of auditory ossicles and hearing loss in mice lacking osteoprotegerin. Bone. 2006; 39(2):414–419. [PubMed: 16564235]
35. Vatsa A, Breuls RG, Semeins CM, Salmon PL, Smit TH, Klein-Nulend J. Osteocyte morphology in fibula and calvaria - Is there a role for mechanosensing? Bone. 2008; 43(3):452–458. [PubMed: 18625577]
36. Seref-Ferlengez Z, Basta-Pljakic J, Kennedy OD, Philomen CJ, Schaffler MB. Structural and Mechanical Repair of Diffuse Damage in Cortical Bone In Vivo. J Bone Miner Res. 2015; 29(12): 2537–3544. [PubMed: 25042459]
37. Kennedy OD, Herman BC, Laudier DM, Majeska RJ, Sun HB, Schaffler MB. Activation of resorption in fatigue-loaded bone involves both apoptosis and active pro-osteoclastogenic signaling by distinct osteocyte populations. Bone. 2012; 50(5):1115–1122. [PubMed: 22342796]

Highlights

- Bone remodeling in cochlea occurs at a very low rate.
- Cochlea preserves hearing despite lack of MMP13.
- Perilacunar remodeling by osteocytes inhibited in cochlea.
- Site-specific regulation of bone remodeling important to consider.

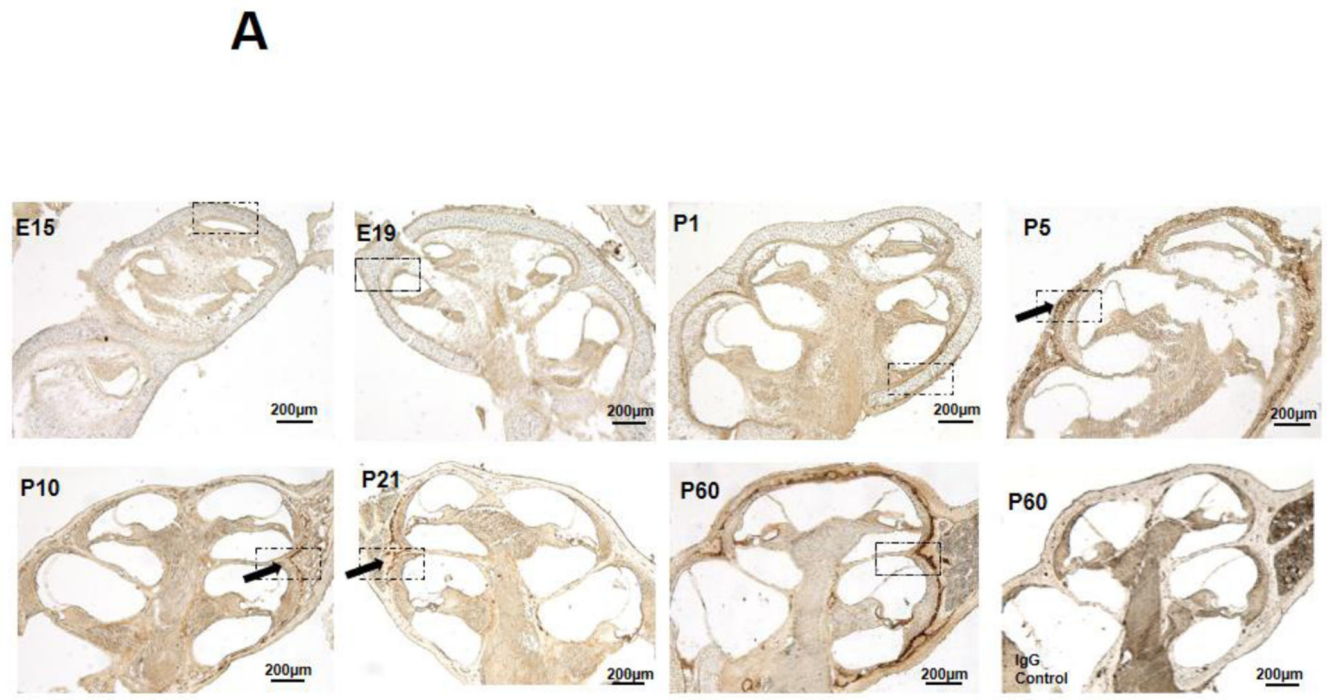

Figure 1a

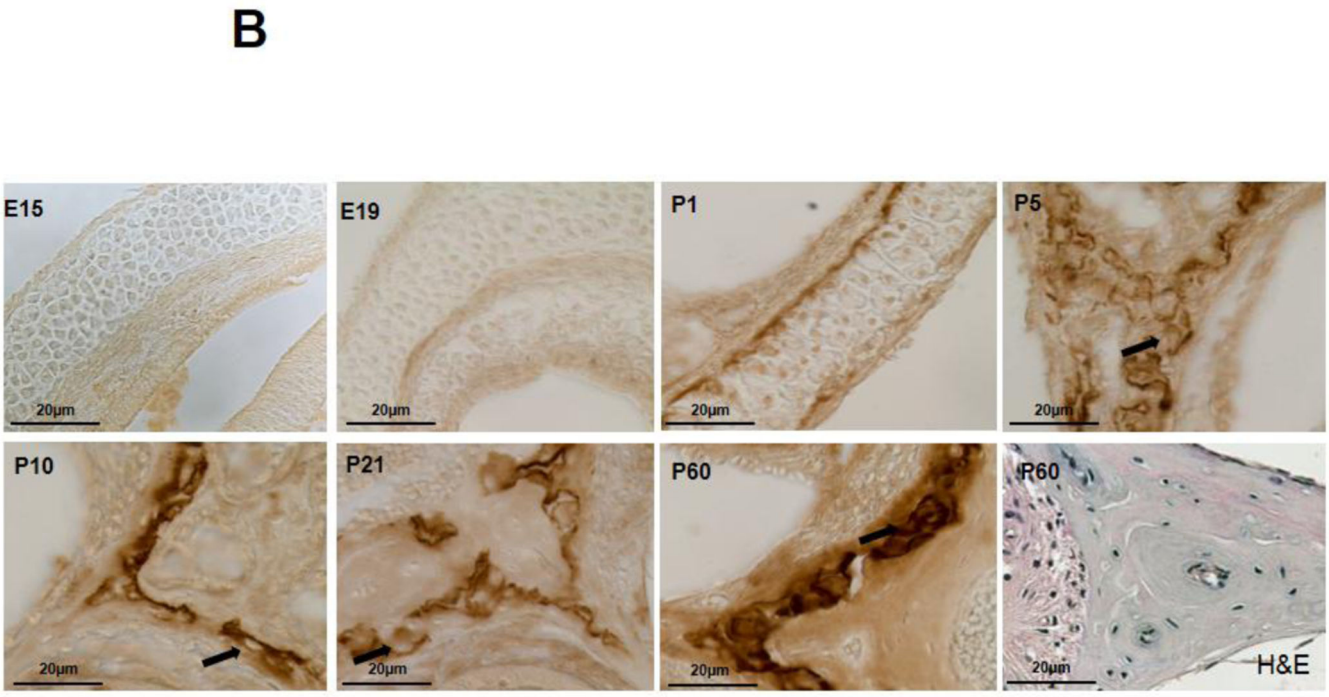

Figure 1b

Figure 1. MMP13 is expressed at multiple stages of development in wild type mouse cochlea

1A. Immunohistochemical staining for MMP13 in WT mouse cochlea at different developmental stages from embryonic-day 15 to post-natal day (p) 60. There are negligible

levels of osteocyte-derived MMP13 from embryonic stages E15 – E19 to immediately after birth (p1). Expression levels rise at p5, during chondrocyte hypertrophy, then, gradually decline to negligible levels in the early p10 to p21 as bone replaces cartilage matrix. It is then re-expressed later in life in the fully developed cochlea, with maximal levels at p60. IgG control stain show small amount of background staining (1A, p60, IgG control). Haematoxylin and eosin stain of cochlear shell (1B, p60 H&E) allows comparison of MMP13 and osteocyte localization in the cochlear shell. Dashed black boxes in Figure 1A indicate the region of interest illustrated in Figure 1B at higher magnification to highlight perilacunar staining. Black arrows indicate areas of perilacunar MMP13 IHC staining. Data from n=3 wild type mice were obtained.

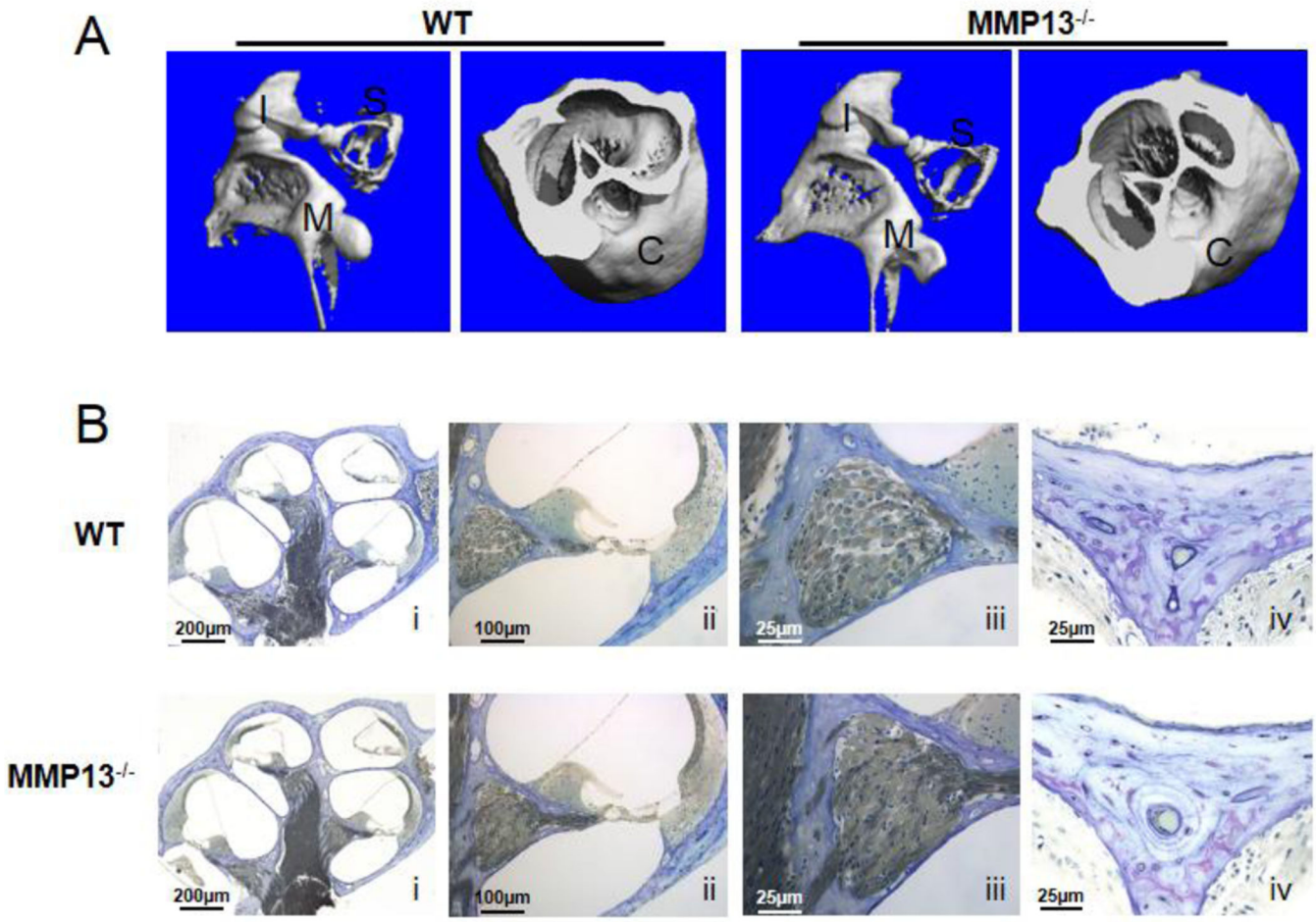

Figure 2. Normal inner ear structures and ossicular chain in wild type and MMP13$^{-/-}$ mice

(A) p60 cochleae were imaged with micro-computed tomography and 3D reconstructed images. The ossicular chain shows no macroscopic deformities suggestive of conductive hearing loss (A; I=incus, S=stapes, M=malleus, C=cochlea). (B) Araldite 502 resin embedded sections stained with toluidine blue of the cochlea obtained from WT (i–iv) and MMP13$^{-/-}$ mice (i–iv) at p60 and examined under light microscopy. No differences were noted within the organ of Corti (ii) or the spiral ganglion (iii). Toluidine blue stains of both WT and MMP13$^{-/-}$ (iv) show no bony deformations. Data from n≥3 wild type mice and n≥3 MMP13$^{-/-}$ mice were obtained.

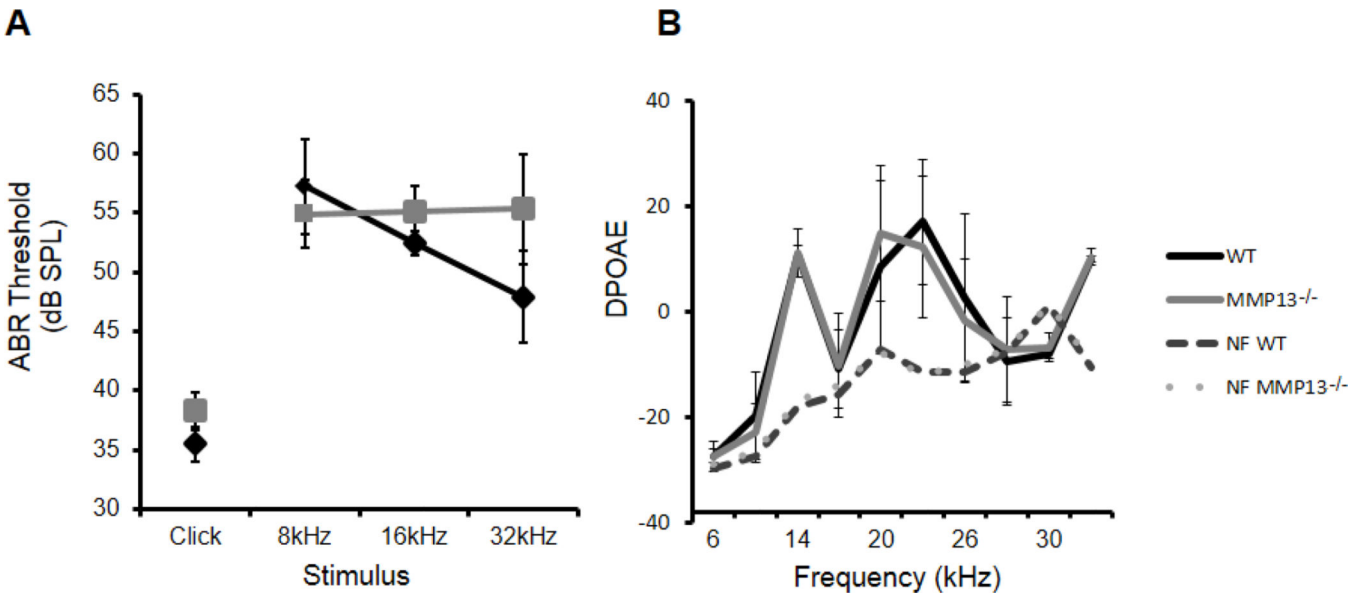

Figure 3. Hearing is maintained despite lack of MMP13

The auditory brainstem responses (ABR) demonstrate no significant difference in thresholds (A) for click stimulus between WT (n=5, 35.5±1.46 dB-SPL) and MMP13$^{-/-}$ (n=10, 38.3±1.58 dB-SPL) mice, at 8kHz (MMP13$^{-/-}$ 54.9±2.81 vs. WT 57.2±4.01 dB-SPL; p>0.05), 16kHz (MMP13$^{-/-}$ 55.0±2.16 vs. WT 52.4±0.99 dB-SPL; p>0.05), or 32kHz frequencies (MMP13$^{-/-}$ 55.3±4.63 vs. WT 47.9±3.84 dB-SPL; p>0.05), error bars are SEM. For DPOAE analysis (B), two-toned stimuli with standard frequency ratio (f_2/f_1=1.25) ranging from 6kHz to 36kHz were presented to the left ear from 55dB to 75dB. Responses in MMP13$^{-/-}$ mice, closely follows that of WT mice and showed no significant difference in functional hearing by two-sample Wilcoxon sum-rank test (p>0.05) (NF = noise floor). Data from n≥3 wild type mice and n≥3 MMP13$^{-/-}$ mice were obtained.

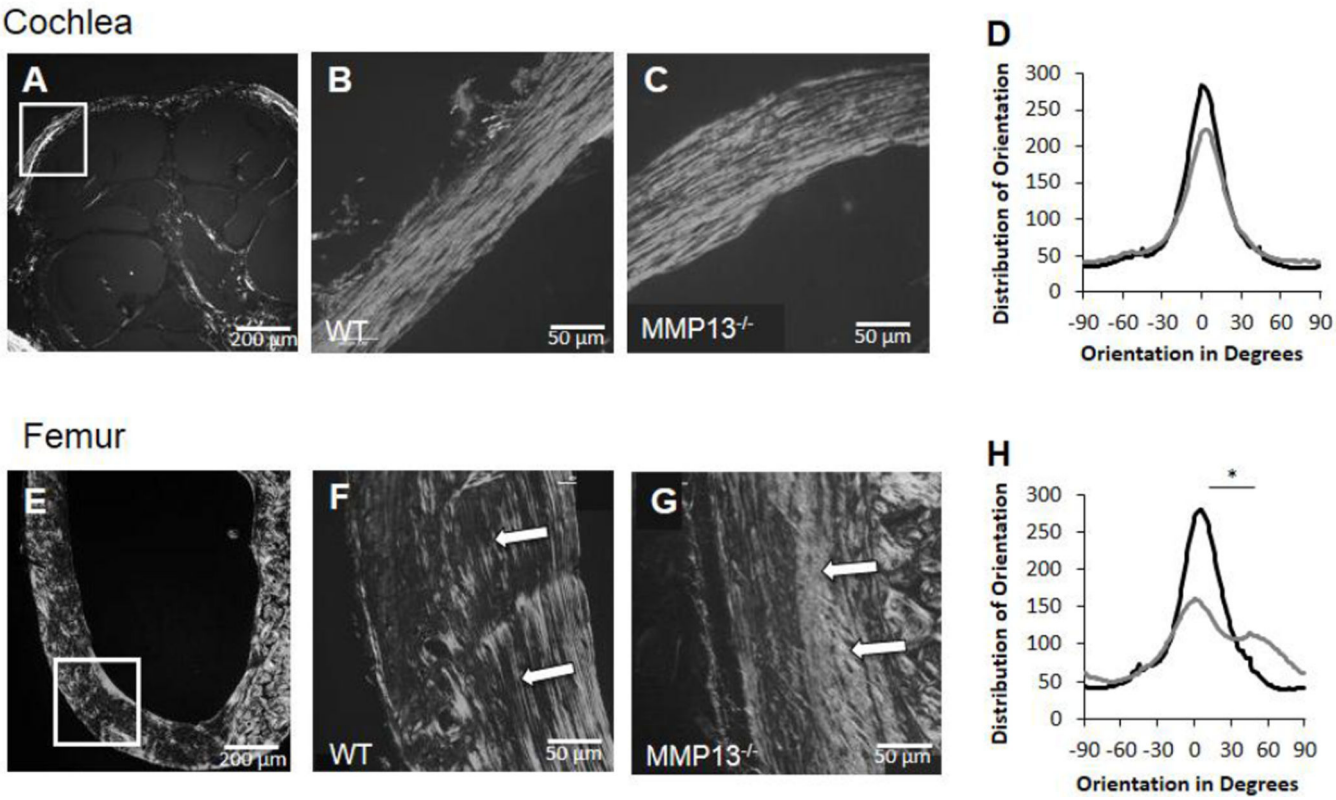

Figure 4. MMP13 is necessary for collagen organization in long bones, not in cochlear bone

Polarized light birefringence after picro-sirius staining of p60 male mice cochleae and femora reveal collagen fibril organization. Both WT and MMP13$^{-/-}$ cochleae reveal well-organized collagen fibrils (A–C, white box indicates region of interest for panels B–C). Plot of the distribution of orientation of collagen fibrils in cochlear bone (D) reveal no differences between MMP13$^{-/-}$ (36.6±10.4°) and WT mice (33.5±7.2°) by histogram analysis of width at half maximum, $p>0.05$, via OrientationJ plug-in for ImageJ. In femora (E–G, white box indicates region of interest for panels F–G), collagen organization is not well organized throughout MMP13$^{-/-}$ mice (G) compared to WT (F). For MMP13$^{-/-}$ femora, the distribution of collagen orientation shows a wider, less well-defined peak (H), suggesting poorer organization by width at half-maximum analysis, (71.8±30.6 vs. 34.3±4.8°, MMP13$^{-/-}$ and WT, respectively; $p=0.0002$). Data from n≥3 wild type mice and n≥3 MMP13$^{-/-}$ mice were obtained.

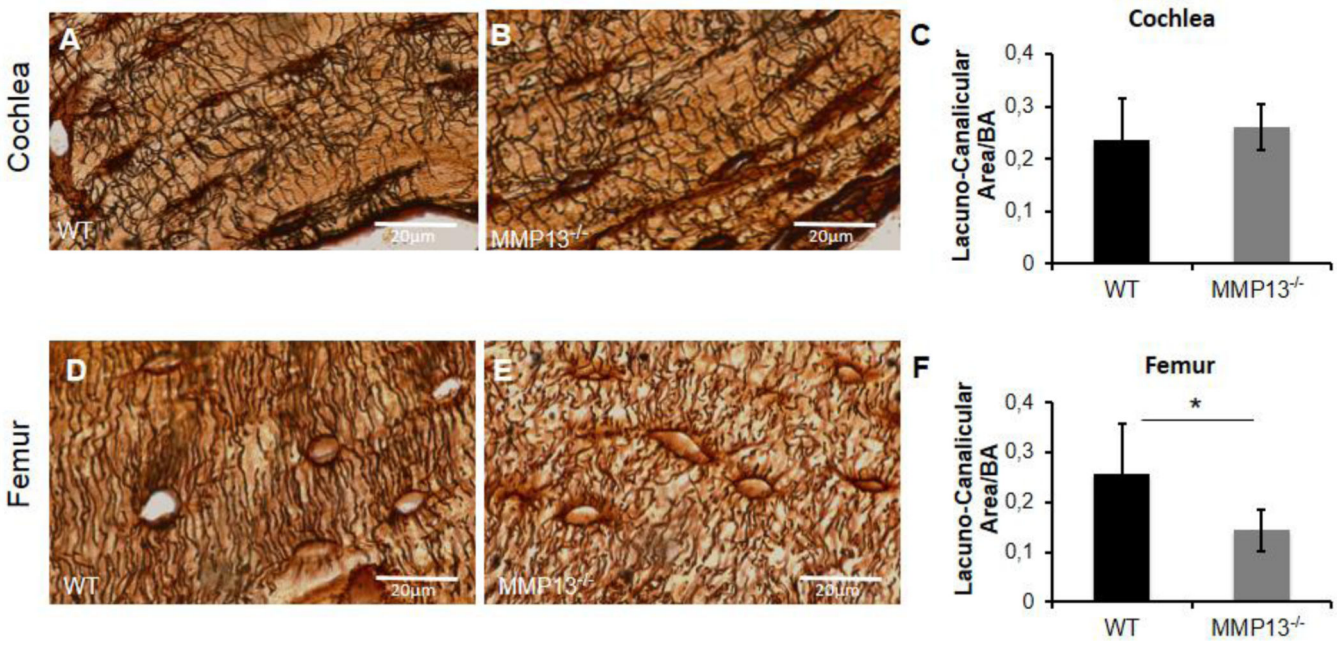

Figure 5. Cochlear canalicular network is maintained without MMP13, however is required in femur

Lacuno-canalicular networks in cochleae (A–B) and femora (D–E) stained with silver nitrate (in black) in male p60 mice. Silver nitrate highlights the lacunae and the radiating canalicular network in cochlea, with no appreciable difference between WT (A) and MMP13$^{-/-}$ mice (B). Quantification of the lacuno-canalicular area, using ImageJ, reveals no significant difference between the two groups (0.260±0.04μm^2 vs. 0.235±0.08μm^2, MMP13$^{-/-}$ and WT, respectively, $p>0.05$) (C). Silver nitrate staining of axial femur section reveals a robust, radiating canalicular network from lacunae in WT femora (D). MMP13$^{-/-}$ mice reveal a less extensive, blunted canalicular network (E). Quantified via ImageJ, MMP13$^{-/-}$ mice have a significantly smaller lacuno-canalicular area (0.143±0.04 μm^2) normalized to bone area, compared to WT mice (0.256±0.10 μm^2; $p=0.0002$) (F). Data was collected from n≥3 cochleae from each group, and from n≥3 MMP13$^{-/-}$ and n=2 wild type mice femora.

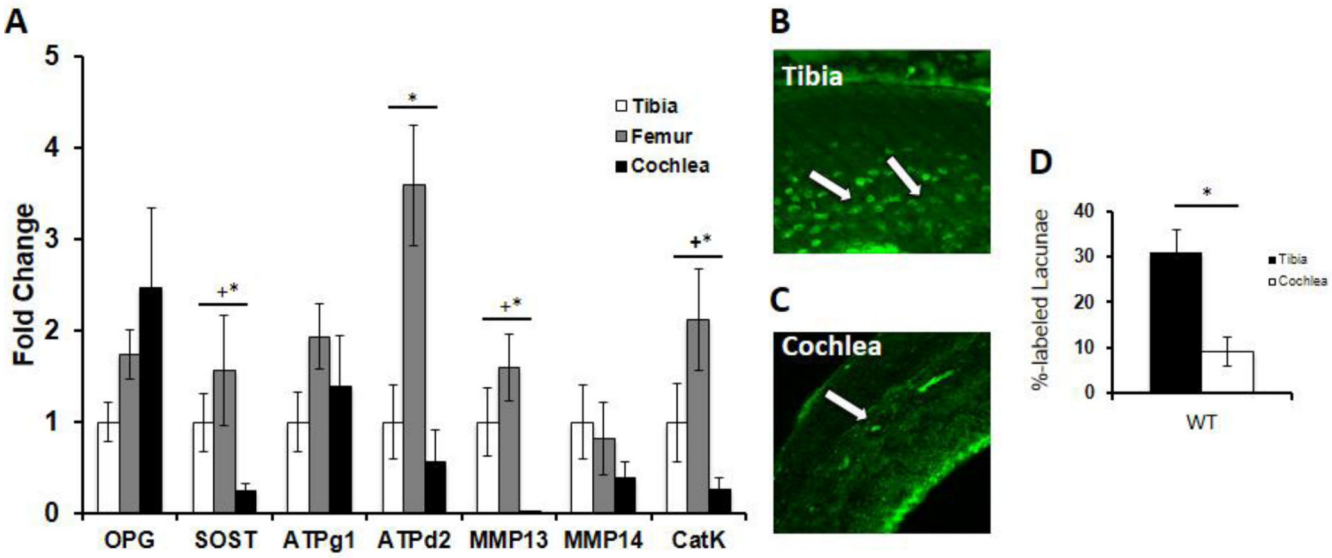

Figure 6. Critical PLR factors are expressed to a lesser degree in the cochlea compared to long bones

(A) qPCR expression levels from p60 WT male mice of osteoprotegerin (OPG), sclerostin (SOST), ATPase H+ transporting lysosomal V0 subunit D2 (ATP6V0D2), ATPase H+ transporting lysosomal V1 subunit G1 (ATP6V1G1), matrix metalloproteinase-13 (MMP13), matrix metalloproteinase-14 (MMP14), and cathepsin-K (CatK) mRNA in cochlea and femur normalized to GAPDH, standardized to levels in the tibia. The relative expression levels of MMP13 and other important PLR genes (CatK, ATPd2, MMP14) in the cochlea are lower than in other bones, suggesting suppressed PLR activity in the cochlea relative to long bones ("+" indicates normalized to tibia, "*" indicates normalized to femur). This is reinforced by quantifying the percentage of calcein labeled lacunae in WT tibia and WT cochlea (D), where tibia revealed 31% labeled lacunae versus 9% in the cochlea (p-value=0.00002). Representative images under confocal microscopy of calcein-stained tibia (B) showing a relatively high number of lacunae with calcein label (Tibia, white arrows) and the relative paucity in cochlea (C) (Cochlea, white arrow). Data was collected from bones from n=3 mice per group.

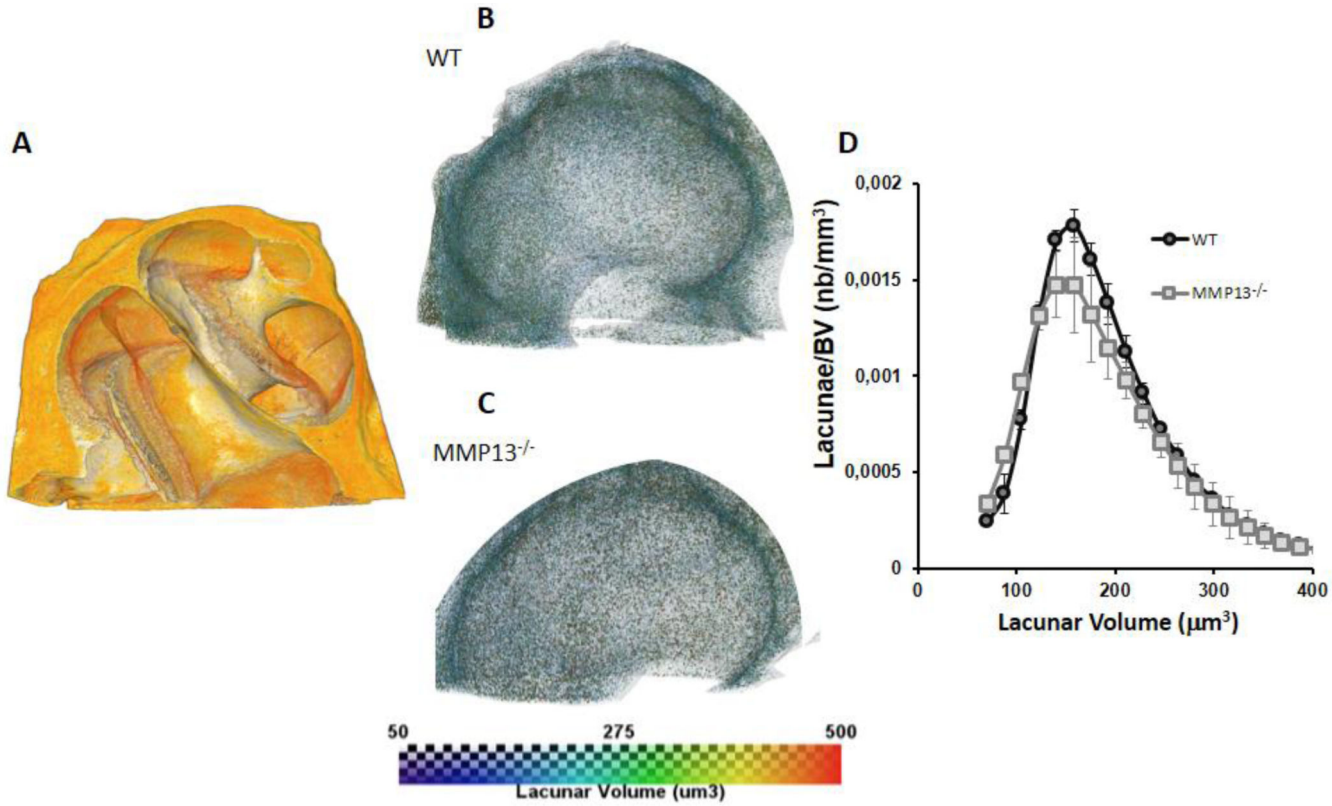

Figure 7. Lacunar volume in cochlear bone is unaffected by MMP13 deficiency

Representative 3D volume rendered image of micro-computed tomography scan of the cochlea (A). Color scale representation of the lacunar volume in μm^3 for WT (B) and $MMP13^{-/-}$ (C). Lacunar volume plotted against number of osteocytes normalized to total bone volume for WT (195.3 $\mu m^3 \pm 59.9$, SEM) and $MMP13^{-/-}$ (192.9 $\mu m^3 \pm 64.1$, SEM) male mice at p60 (D). The two groups showed no significant differences in the average lacunar volumes in the cochlea despite the lack of MMP13 as seen by similar histogram shapes and by Wilcoxon rank sum test, ($p>0.05$) (nb = number). Data from n=3 wild type mice and n=3 $MMP13^{-/-}$ mice were obtained.